

Dimming Space-Time Code (DSTC) for Visible Light Communication with Semi-Blind Detection

Igor S. C. Rodrigues, Leandro R. Ximenes e André L. F. de Almeida

Abstract—Visible light communication (VLC) provides a unified framework for wireless data transmission and illumination, but its practical deployment requires transmission schemes that jointly satisfy communication and lighting constraints. In color-shift keying (CSK) systems, dimming remains a challenging and underexplored problem because the average optical power must be controlled without altering the perceived chromaticity. This paper proposes a dimming space-time code (DSTC) for CSK-based VLC systems, in which a structured dimming matrix introduces controlled temporal power variations while satisfying physical feasibility, color-preservation, and identifiability conditions. Two receiver architectures are developed: a pilot-assisted zero-forcing (ZF) receiver and a tensor-based semi-blind PARAFAC receiver that jointly estimates the channel and transmitted symbols using only one training time slot. Simulation results show that the proposed DSTC provides diversity gains and substantial BER reductions with respect to conventional CSK, while the tensor-based receiver improves spectral efficiency by reducing training overhead, with particular benefits in large-scale MIMO configurations.

Keywords—Visible Light Communication, color-shift keying, dimming control, tensor modeling.

I. INTRODUCTION

Visible light communication (VLC) has emerged as a promising technology for simultaneous wireless data transmission and illumination by exploiting the unlicensed visible-light spectrum. In comparison with radio-frequency (RF) systems, VLC can provide high data rates, low-cost implementation, spatial confinement, and enhanced physical-layer security [1]. Since VLC transmitters are also illumination sources, communication design must account for lighting constraints in addition to conventional reliability and spectral-efficiency requirements. In particular, dimming control, i.e., the adjustment of the average optical power emitted by the LEDs, is required to satisfy user comfort and energy-efficiency targets while avoiding perceptible flicker and performance degradation [2]. Most existing dimming techniques have been developed for intensity-modulation/direct-detection (IM/DD) schemes such as on-off keying (OOK) and pulse-position modulation (PPM), where dimming is typically implemented through duty-cycle adaptation or symbol-probability shaping [3]–[6].

Igor Cruz, Universidade Federal do Ceará, UFC, Fortaleza-CE, e-mail: i263014@dac.unicamp.br; Leandro Ximenes, Faculdade de Tecnologia, UNICAMP, Limeira-SP, e-mail: leandro@ft.unicamp.br; André L. F. de Almeida, Universidade Federal do Ceará, UFC, Fortaleza-CE, e-mail: andre@gtel.ufc.br. This work is partially supported by the National Institute of Science and Technology (INCT-Signals) sponsored by Brazil's National Council for Scientific and Technological Development (CNPq) (Proc. 406517/2022-3), and FUNCAP (Proc. INCT-25255-82587.32.41/64). The research of André L. F. de Almeida is partially supported by CNPq (Proc. 303356/2025-1).

Color-shift keying (CSK) conveys information by controlling the relative optical intensities of LEDs with distinct chromatic components, so that data symbols are represented by points in a chromaticity diagram [2]. This modulation principle is attractive for VLC because it enables illumination with reduced flicker and improved energy efficiency. However, dimming in CSK systems is more constrained than in scalar IM/DD schemes: the average optical power must be adjusted without perturbing the target chromaticity perceived by the user. Consequently, dimming control for CSK remains relatively underexplored, especially in multiple-input multiple-output (MIMO) configurations. The multidimensional design of CSK-based MIMO-VLC systems, potentially involving spatial, temporal, and chromatic dimensions, suggests that dimming can also be incorporated into the transmission code as an additional degree of freedom. In this perspective, controlled power variations across LEDs and time slots can provide diversity while preserving the average emitted color. Existing CSK diversity schemes, such as the color-hopping space-time (CHST) code in [7], exploit color, spatial, and temporal diversity, but they do not explicitly formulate dimming as a coding dimension nor address the corresponding receiver structure.

Tensor modeling provides a rigorous algebraic framework for communication systems whose signals are naturally indexed by multiple coupled dimensions. Parallel factor analysis (PARAFAC) and related tensor decompositions have been widely used for blind and semi-blind receiver design, multiuser equalization, constrained MIMO factorization, space-time-frequency coding, and reconfigurable-surface-assisted systems, benefiting from identifiability properties that can reduce training overhead [8]–[18]. These properties are particularly relevant for CSK-based VLC with dimming codes, because the received signal can be represented through coupled spatial, temporal, and chromatic factors associated with the channel, the transmitted symbols, and the dimming pattern.

Motivated by these observations, this paper proposes a dimming space-time code (DSTC) for CSK-based VLC systems. The proposed code introduces controlled temporal variations in optical power through a dimming matrix that satisfies physical nonnegativity, average-power, chromaticity-preservation, and rank conditions. Unlike conventional dimming approaches, the proposed DSTC uses dimming not only as an illumination-control mechanism but also as a source of transmission diversity. Moreover, two receiver strategies are developed: a pilot-based zero-forcing (ZF) receiver and a semi-blind tensor receiver based on PARAFAC/Khatri–Rao factorization, which jointly estimates the channel and transmitted symbols

with only one training time slot. To the best of the authors' knowledge, this is the first work to exploit dimming as a diversity dimension in CSK-based VLC and to introduce a tensor-based semi-blind receiver for this class of systems.

The remainder of this paper is organized as follows. Section 2 presents the proposed DSTC signal model and dimming-pattern design. Section 3 derives the ZF and tensor-based receivers. Section 4 discusses the simulation results, including bit-error-rate, channel-estimation, and spectral-efficiency comparisons. Finally, Section 5 concludes the paper.

II. DIMMING SPACE-TIME CODE (DSTC)

Consider a point-to-point multiple-input multiple-output (MIMO) VLC block-transmission system employing CSK modulation under a linear intensity-modulation/direct-detection (IM/DD) channel model. The transmitter consists of L_T LED groups, each containing K_T color channels, yielding a total of $K_T L_T$ transmit optical sources. The symbol matrix $\mathbf{S} \in \mathbb{R}^{N \times K_T L_T}$ contains a block of N CSK symbols multiplexed across these optical sources. For instance, in the QuadLED (QLED) architecture proposed in [19], $K_T = 4$ color channels are considered. The goal of the proposed DSTC scheme is to impose controlled temporal variations on the instantaneous optical power while preserving the prescribed average color and illumination level. This is accomplished through a dimming matrix \mathbf{C} , whose entries scale the optical intensity emitted by each LED at each transmission state. As illustrated in Fig. 1, the dimming block therefore introduces an additional temporal coding dimension that can be exploited for diversity without changing the average chromaticity perceived by the receiver.

Assume that the block of N symbols in \mathbf{S} is transmitted over K dimming states. The dimming matrix $\mathbf{C} \in \mathbb{R}^{K \times K_T L_T}$ is defined such that its k -th row specifies the normalized dimming coefficients applied to all transmit LEDs during the k -th state. Let $\Psi_k(\mathbf{C}) \in \mathbb{R}^{K_T L_T \times K_T L_T}$ denote the diagonal matrix obtained from the k -th row of \mathbf{C} , i.e.,

$$\Psi_k = \text{diag}(C_{k,1}, C_{k,2}, \dots, C_{k,K_T L_T}). \quad (1)$$

The transmitted signal matrix at the k -th dimming state is

$$\mathbf{X}_k = \Psi_k \mathbf{S}^T, \quad (2)$$

where $\mathbf{X}_k \in \mathbb{R}^{K_T L_T \times N}$. Thus, the coefficients in Ψ_k scale the instantaneous optical power of each LED, whereas the design of \mathbf{C} enforces the desired average illumination and chromaticity over the complete set of K states.

Fig. 1 illustrates the DSTC principle for a single-input single-output (SISO) configuration ($L_R = L_T = 1$) using triLED (TLED) transmitters and receivers ($K_R = K_T = 3$).

A. Dimming Pattern Design

The dimming matrix \mathbf{C} must satisfy two sets of requirements: physical feasibility constraints and an algebraic rank condition.

1) *Physical constraints*: Since the entries of \mathbf{C} represent normalized optical-intensity scaling factors under an IM/DD model, they must satisfy

$$0 \leq C_{k,i} \leq 1, \quad \forall k, i, \quad (3)$$

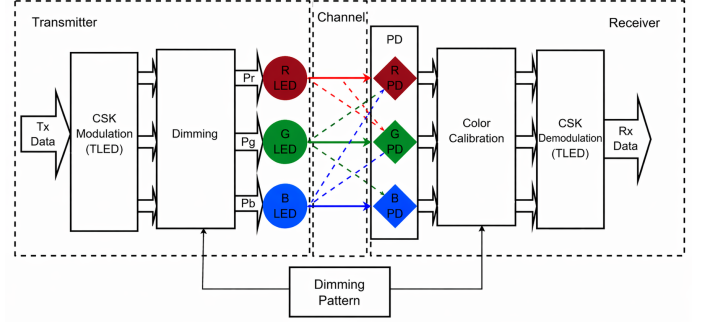


Fig. 1: Proposed DSTC transmission scheme for a SISO TLED/CSK VLC system.

where $i = 1, \dots, K_T L_T$ indexes the transmit LEDs. In addition, to impose a prescribed average optical power per LED, the coefficients must satisfy

$$\frac{1}{K} \sum_{k=1}^K C_{k,i} = P_m, \quad \forall i, \quad (4)$$

where P_m denotes the target normalized dimming level. The perceived color of illumination must also remain invariant on average. The resulting chromaticity coordinates are given by

$$x = \sum_{k_t=1}^{K_T} P_{k_t} x_{k_t}, \quad y = \sum_{k_t=1}^{K_T} P_{k_t} y_{k_t}, \quad (5)$$

where (x_{k_t}, y_{k_t}) are the CIE 1931 chromaticity coordinates of the k_t -th color channel and P_{k_t} denotes its average transmitted optical power after dimming. Hence, \mathbf{C} must be designed so that dimming changes the average optical power while preserving the target chromaticity.

textit2) Rank condition: From an algebraic viewpoint, \mathbf{C} must have full column rank, i.e.,

$$\text{rank}(\mathbf{C}) = K_T L_T. \quad (6)$$

This condition requires $K \geq K_T L_T$ and ensures that the temporal dimming signatures assigned to different LEDs are linearly independent. It also guarantees the existence of a left pseudoinverse of \mathbf{C} , which is required by the proposed receiver architectures to separate the contributions from the different transmit optical sources.

B. Construction of \mathbf{C} via Hadamard Matrix

A structured construction satisfying the above requirements can be obtained from a Hadamard matrix. Specifically, define

$$\mathbf{C} = P_m \mathbf{1}_{K \times K_T L_T} + \alpha \mathbf{B}, \quad (7)$$

where $\mathbf{1}_{K \times K_T L_T}$ is an all-ones matrix and $\mathbf{B} \in \mathbb{R}^{K \times K_T L_T}$ is formed by selecting columns from a Hadamard matrix of order K , with entries in $\{-1, +1\}$. The scalar α controls the amplitude of the temporal power variations around the average dimming level P_m .

One possible construction is to select $K_T L_T$ nonconstant columns from a Hadamard matrix of order K , excluding the all-ones column. These selected columns have zero sample mean, i.e., $\sum_{k=1}^K B_{k,i} = 0$, which directly enforces (4). Since

at most $K - 1$ nonconstant Hadamard columns are available, this construction requires $K_T L_T \leq K - 1$. In addition, standard Hadamard matrices exist for orders satisfying $K = 1$, $K = 2$, or $K \pmod{4} = 0$; in the present design, K is chosen so that a suitable order- K Hadamard matrix is available. To ensure nonnegative and bounded optical intensities, α must satisfy

$$\alpha \leq \min(P_m, 1 - P_m), \quad (8)$$

which ensures (3) since each entry of \mathbf{C} lies in $\{P_m - \alpha, P_m + \alpha\}$. The zero-mean property of these Hadamard columns guarantees (4), whereas their mutual orthogonality ensures (6).

III. SYMBOL DETECTION

This section presents the proposed receiver architectures for symbol detection in the DSTC scheme. First, we describe a conventional *zero-forcing* (ZF) receiver based on pilot-assisted channel estimation. We then introduce a tensor-based semi-blind receiver that exploits the PARAFAC structure of the received signal, enabling joint channel and symbol estimation with reduced training overhead. At the receiver, L_R groups of K_R photodetectors are employed. The received signal associated with the k -th dimming state is obtained by transmitting the signal in (2) through the wireless optical channel, yielding

$$\mathbf{Y}_k = \mathbf{H}_k \mathbf{X}_k = \mathbf{H}_k \Psi_k \mathbf{S}^T + \mathbf{N}_k, \quad (9)$$

where $\mathbf{H}_k \in \mathbb{R}^{K_R L_R \times K_T L_T}$ denotes the channel matrix, \mathbf{N}_k is the additive white Gaussian noise (AWGN) matrix, and $\mathbf{Y}_k \in \mathbb{R}^{K_R L_R \times N}$ denotes the received symbol matrix.

A. Zero-Forcing Receiver

For the ZF receiver, the K received blocks in (9) are stacked into the concatenated matrix $\bar{\mathbf{Y}} \in \mathbb{R}^{K_R L_R K \times N}$, defined as

$$\bar{\mathbf{Y}} = \left[(\mathbf{H}_1 \Psi_1)^T \cdots (\mathbf{H}_K \Psi_K)^T \right]^T \mathbf{S}^T + \mathbf{N}. \quad (10)$$

From this, the effective channel matrix \mathbf{H}_e is defined as

$$\mathbf{H}_e = \text{blkdiag}(\mathbf{H}_1, \mathbf{H}_2, \dots, \mathbf{H}_K) [\Psi_1^T \Psi_2^T \cdots \Psi_K^T]^T, \quad (11)$$

where $\text{blkdiag}(\cdot)$ denotes a block-diagonal matrix. Substituting (11) into (10), the received signal model can be rewritten as

$$\bar{\mathbf{Y}} = \mathbf{H}_e \mathbf{S}^T + \mathbf{N}. \quad (12)$$

Channel estimation can be performed by transmitting a pilot sequence before data transmission. Assuming the channel remains constant across the K dimming states, a simple strategy is to activate one LED at a time at maximum power while keeping the others off during each time slot. This procedure requires $K_T L_T$ pilot time slots, which reduces spectral efficiency and effective throughput.

The pilot symbol sequence is known a priori at both the transmitter and the receiver and is defined by the matrix \mathbf{S}_0 . Using (12), the receiver estimates the channel matrix as

$$\hat{\mathbf{H}}_e \triangleq \tilde{\mathbf{Y}}_0 (\mathbf{S}_0^T)^\dagger, \quad (13)$$

where $\tilde{\mathbf{Y}}_0$ is the set of received signals during the channel estimation phase, and \dagger represents the Moore–Penrose pseudoinverse. Since the dimming matrix \mathbf{C} is also known at the

receiver, an equalizer can be applied to estimate \mathbf{S} from (12) and (13). The resulting ZF equalizer is given by

$$\hat{\mathbf{S}} = (\hat{\mathbf{H}}_e^\dagger \tilde{\mathbf{Y}})^T. \quad (14)$$

B. Semi-Blind Tensor-Based Channel and Symbol Estimator

Alternatively, the received data can be rearranged into a third-order tensor model, enabling semi-blind joint channel and symbol estimation through the PARAFAC decomposition originally introduced in [20]. Using the identity

$$\text{vec}(\mathbf{A}\mathbf{X}\mathbf{B}) = (\mathbf{B}^T \otimes \mathbf{A}) \text{vec}(\mathbf{X}), \quad (15)$$

and assuming that the channel remains constant over K dimming states, the vectorized received signal is given by

$$\mathbf{y}_k = (\mathbf{S} \otimes \mathbf{H}) \text{vec}(\Psi_k) \in \mathbb{R}^{K_R L_R N \times 1}. \quad (16)$$

Since Ψ_k is diagonal, it follows that

$$(\mathbf{S} \otimes \mathbf{H}) \text{vec}(\Psi_k) = (\mathbf{S} \diamond \mathbf{H}) \mathbf{c}_k^T, \quad (17)$$

where \mathbf{c}_k denotes the k -th row of \mathbf{C} . Thus,

$$\mathbf{y}_k = (\mathbf{S} \diamond \mathbf{H}) \mathbf{c}_k^T. \quad (18)$$

Finally, stacking all dimming states yields

$$\mathbf{Y}_{(3)} = [\mathbf{y}_1^T \mathbf{y}_2^T \cdots \mathbf{y}_K^T]^T = \mathbf{C}(\mathbf{S} \diamond \mathbf{H})^T \in \mathbb{R}^{K \times K_R L_R N}. \quad (19)$$

This structure naturally leads to the PARAFAC decomposition

$$\mathcal{Y} = \llbracket \mathbf{H}, \mathbf{S}, \mathbf{C} \rrbracket \in \mathbb{R}^{K_R L_R \times N \times K}. \quad (20)$$

The three modes correspond, respectively, to receiver elements, transmitted symbols, and dimming states. The PARAFAC structure yields the following unfoldings of \mathcal{Y} :

$$\mathbf{Y}_{(1)} = \mathbf{H}(\mathbf{C} \diamond \mathbf{S})^T \in \mathbb{R}^{K_R L_R \times NK}, \quad (21)$$

$$\mathbf{Y}_{(2)} = \mathbf{S}(\mathbf{C} \diamond \mathbf{H})^T \in \mathbb{R}^{N \times K_R L_R K}, \quad (22)$$

$$\mathbf{Y}_{(3)} = \mathbf{C}(\mathbf{S} \diamond \mathbf{H})^T \in \mathbb{R}^{K \times K_R L_R N}. \quad (23)$$

1) *Uniqueness Conditions:* For the tensor model to be identifiable, and hence enable semi-blind joint channel and symbol estimation, the PARAFAC decomposition must be essentially unique up to permutation and scaling.

Proposition 1: Assume that \mathbf{S} has full column rank and that \mathbf{C} is constructed according to (7). Then, (20) is essentially unique if $k_H \geq 2$, where k_H is the Kruskal rank of \mathbf{H} .

Proof 1: According to Kruskals condition [21], for a model of rank $R = K_T L_T$, it holds that $k_H + k_S + k_C \geq 2R + 2$. Since \mathbf{S} has full column rank for sufficiently large N , we have $k_S = K_T L_T$. Moreover, because \mathbf{C} is constructed from distinct columns of a Hadamard matrix as in (7), it also has full column rank, yielding $k_C = K_T L_T$. Therefore, the condition reduces to $k_H \geq 2$, which ensures essential uniqueness.

Remark 1: While the ZF receiver requires $K_R L_R \geq K_T L_T$, the tensor-based approach only requires that no two rows of \mathbf{H} be linearly dependent. Under the commonly adopted VLC assumption of negligible optical crosstalk, \mathbf{H} is approximately diagonal, which naturally satisfies this requirement even in scenarios with fewer receivers than transmitters.

Proposition 2: If $N < K_T L_T$ and $K_R L_R > K_T L_T$, then $k_S \geq 2$ is sufficient for essential uniqueness.

Algorithm 1 VLC-KRF

Require: $\tilde{\mathcal{Y}}, \mathbf{C}, \mathbf{S}_n$

- 1: $\tilde{\mathbf{Y}}^{(3)} \leftarrow \text{mode-3 unfolding of } \tilde{\mathcal{Y}}$
- 2: $\mathbf{Q} = \tilde{\mathbf{Y}}^{(3)} (\mathbf{C}^T)^\dagger \approx \mathbf{S} \diamond \mathbf{H}$
- 3: **for** $r = 1, \dots, K_T L_T$ **do**
- 4: $\mathbf{Q}_r = \text{unvec}_{K_R L_R \times N}(\mathbf{q}_r)$
- 5: $[\mathbf{U}, \mathbf{\Sigma}, \mathbf{V}] = \text{svd}(\mathbf{Q}_r)$
- 6: $\hat{\mathbf{h}}_r = \mathbf{U}_{:,1}, \quad \hat{\mathbf{s}}_r = \mathbf{V}_{:,1}$
- 7: **end for**
- 8: $\mathbf{\Delta} = \mathbf{S}_n ./ \hat{\mathbf{S}}_n$
- 9: $\hat{\mathbf{S}} \leftarrow \hat{\mathbf{S}} \mathbf{\Delta}, \quad \hat{\mathbf{H}} \leftarrow \hat{\mathbf{H}} \mathbf{\Delta}^{-1}$

Ensure: $\hat{\mathbf{H}}, \hat{\mathbf{S}}$

Proof 2: \mathbf{H} has full column rank since it is a diagonal matrix with more rows than columns, yielding $k_H = K_T L_T$. Similarly, \mathbf{C} has full column rank by construction, resulting in $k_C = K_T L_T$. Applying Kruskals condition leads to $k_S \geq 2$.

2) *Khatri-Rao Factorization (VLC-KRF):* Once the PARA-FAC structure is shown to be identifiable, the channel and symbol matrices can be jointly estimated through Khatri-Rao factorization. From the mode-3 unfolding in (23), we obtain

$$\mathbf{Q} = (\mathbf{Y}_{(3)})^T (\mathbf{C}^T)^\dagger = (\mathbf{S} \diamond \mathbf{H}). \quad (24)$$

The objective is to factorize each column $\hat{\mathbf{q}}_r$, with $r = 1, \dots, K_T L_T$, as the Khatri-Rao product of two vectors $\hat{\mathbf{s}}_r$ and $\hat{\mathbf{h}}_r$, such that $\hat{\mathbf{q}}_r \approx \hat{\mathbf{s}}_r \otimes \hat{\mathbf{h}}_r = \text{vec}(\hat{\mathbf{h}}_r \hat{\mathbf{s}}_r^T)$. Let \mathbf{Q}_r denote the reshaped version of $\hat{\mathbf{q}}_r$, defined as $\mathbf{Q}_r = \text{unvec}_{K_R L_R \times N}(\hat{\mathbf{q}}_r) \approx \mathbf{h}_r \mathbf{s}_r^T$. Therefore, recovering \mathbf{h}_r and \mathbf{s}_r amounts to solving a rank-one approximation problem:

$$\min_{\mathbf{h}_r, \mathbf{s}_r} \|\mathbf{Q}_r - \mathbf{h}_r \mathbf{s}_r^T\|_F^2, \quad (25)$$

which can be solved using the SVD. Algorithm 1 summarizes the proposed VLC-KRF receiver. For an arbitrary n , the scaling ambiguity is resolved using the diagonal matrix $\mathbf{\Delta}$ given by $\mathbf{\Delta} \approx (\mathbf{S}_n) ./ (\hat{\mathbf{S}}_n)$, $\hat{\mathbf{S}} \leftarrow \hat{\mathbf{S}} \mathbf{\Delta}$, $\hat{\mathbf{H}} \leftarrow \hat{\mathbf{H}} \mathbf{\Delta}^{-1}$, where \mathbf{S}_n is a known row of the transmitted symbol matrix. Therefore, the tensor model requires only a single known row of \mathbf{S} , reducing the training sequence from $K_T L_T$ time slots in the ZF receiver to a single time slot.

C. Spectral Efficiency

For a 4-CSK system, each symbol conveys $\log_2(4) = 2$ bits. Considering L_T transmitters and N distinct symbols per block, the total number of useful transmitted bits is $2L_T N$. Since the K transmission blocks correspond to repetitions of the same symbols, they only increase the transmission time.

For the ZF and VLC-KRF receivers, the spectral efficiencies are given by

$$\eta_{\text{ZF}} = \frac{2L_T N}{NK + K_T L_T}, \quad (26)$$

$$\eta_{\text{VLC-KRF}} = \frac{2L_T N}{NK + 1}. \quad (27)$$

Thus, the spectral-efficiency gain of VLC-KRF is exclusively due to the reduced training overhead:

$$\frac{\eta_{\text{VLC-KRF}}}{\eta_{\text{ZF}}} = \frac{NK + K_T L_T}{NK + 1}. \quad (28)$$

TABLE I: Average power and color before and after dimming ($K_T=3, L_T=2, K=12$)

Metric	Before	After
Power	1	0.5001
Color (x, y)	(0.4389, 0.2910)	(0.4389, 0.2909)

Therefore, the advantage of the tensor-based receiver is more pronounced for small values of NK , whereas both receivers achieve similar efficiencies as NK increases.

IV. RESULTS AND DISCUSSION

The channel \mathbf{H} is modeled as a Gaussian random matrix that remains constant over the K transmission blocks and is corrupted by AWGN. BER results are obtained through Monte Carlo simulations using 10^5 equiprobable 4-CSK symbols transmitted in blocks of $N = 100$ symbols. Unless otherwise stated, $P_m = 0.5$ and $\alpha = 0.4$. Table I compares the average transmitted color and average transmitted power before and after applying the DSTC scheme. The average transmitted color is computed using (5). The results show that the proposed scheme achieves the desired dimming level without altering the average transmitted color, with variations remaining below the typical perceptual sensitivity predicted by Weber's law.

Fig. 2a shows the BER for different values of K . Increasing it provides diversity and coding gains, enabling a BER of 10^{-4} at approximately 24 dB, whereas conventional CSK does not reach 10^{-3} even at 60 dB. For $K = 12$, the ZF receiver provides an additional gain of nearly 10 dB over VLC-KRF, at the cost of lower spectral efficiency since it requires $K_T L_T$ pilot time slots for channel estimation. Increasing K also introduces more temporal diversity, but reduces throughput.

Fig. 2b shows the normalized mean-square error (NMSE) of channel estimation for both proposed receivers. The VLC-KRF receiver achieves a lower channel-estimation error than the ZF receiver, which is particularly relevant for applications that require accurate channel knowledge, such as visible light positioning. The final simulation evaluates the impact of the parameter α , which controls the peak-to-average power ratio of the transmitted signal. A QLED 2×2 system with $K = 12$, $P_m = 0.5$, and SNR of 20 dB is considered. The BER performance of both proposed receivers is compared. From a perceptual standpoint, if the modulation rate is sufficiently high - that is, above the flicker-fusion threshold, typically on the order of 100-200 Hz [22] - these power variations are not perceptible to the human eye, which integrates the received light and perceives a constant illumination proportional to the average optical power. As shown in Fig. 3, increasing α improves the performance of both receivers by improving the conditioning of the dimming matrix \mathbf{C} and of the effective channel. The average condition number decreases from 20.9169 for $\alpha = 0.1$ to 9.2635 for $\alpha = 0.5$. The ZF receiver benefits more from this improvement because it explicitly relies on effective channel inversion, whereas VLC-KRF is more robust due to its SVD-based factorization.

Table II compares the spectral efficiencies of both receivers for different scenarios using the equations (26)-(28). The gain increases with the number of transmit arrays and decreases as K increases, indicating that the tensor-based VLC-KRF

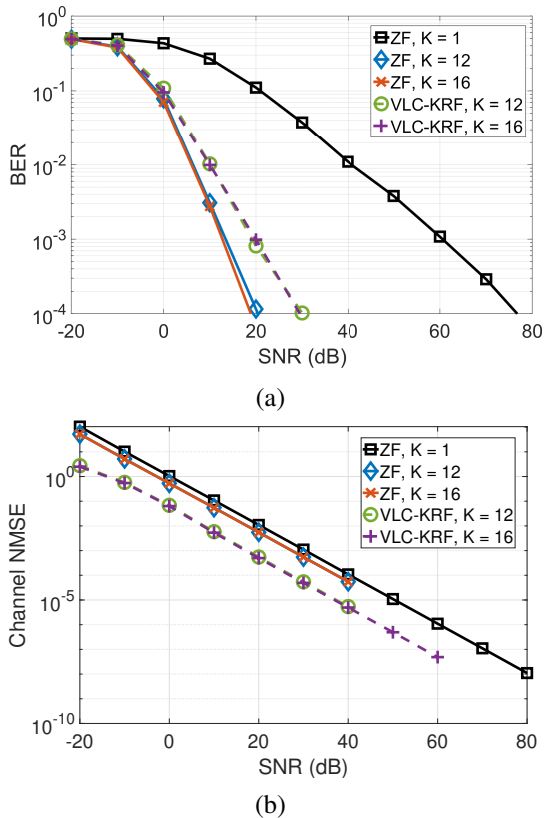
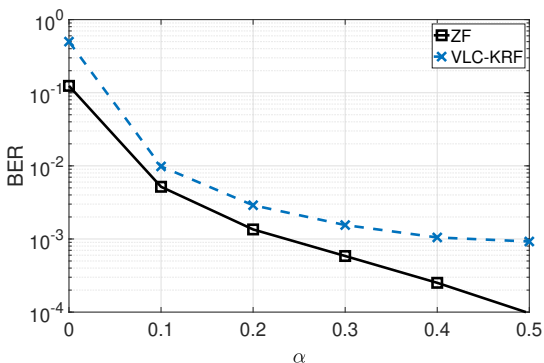

 Fig. 2: BER and NMSE for the QLED MIMO 2×2 system.

 Fig. 3: BER for different α values in a QLED 2×2 system.

 TABLE II: Spectral efficiency for different configurations ($N = 10$)

Case	$K_T L_T$	K	η_{ZF}	$\eta_{VLC-KRF}$	Gain (%)	Scenario
1	6	8	0.4651	0.4938	6.1	$K_T=3, L_T=2$
2	18	20	0.5505	0.5970	8.4	$K_T=3, L_T=6$
3	30	32	0.5714	0.6231	9.0	$K_T=3, L_T=10$
4	8	12	0.3125	0.3306	5.8	$K_T=4, L_T=2$
5	8	16	0.2381	0.2484	4.3	$K_T=4, L_T=2$

receiver is more advantageous for large-scale MIMO systems, whereas the ZF receiver may offer better performance in smaller MIMO scenarios with a lower spectral-efficiency penalty.

V. CONCLUSION

This work proposed a DSTC for VLC systems based on CSK modulation, exploiting the multidimensional structure of the problem to enable illumination control while preserving

color and satisfying physical constraints. The proposed framework supports two receivers: a ZF receiver with pilot-based estimation and a tensor-based receiver that performs semi-blind joint estimation via PARAFAC. The results demonstrated increased diversity and a significant reduction in BER compared with conventional CSK. In addition, the tensor-based receiver achieved lower channel-estimation error and higher spectral efficiency by reducing training overhead to a single time slot, making it particularly attractive in scenarios with more transmitters. Future work includes investigating codes that jointly exploit color diversity and dimming, as well as exploring alternative tensor models for this scenario.

REFERENCES

- [1] D. C. O'Brien, L. Zeng, H. Le-Minh, G. Faulkner, J. W. Walewski, and S. Randel, "Visible light communications: Challenges and possibilities," in *2008 IEEE 19th Int. Symp. on Pers., Indoor and Mobile Radio Commun.*, 2008, pp. 1–5.
- [2] S. Rajagopal, R. D. Roberts, and S.-K. Lim, "IEEE 802.15.7 visible light communication: Modulation schemes and dimming support," *IEEE Commun. Mag.*, vol. 50, no. 3, pp. 72–82, 2012.
- [3] K. Lee and H. Park, "Modulations for visible light communications with dimming control," *IEEE Photon. Technol. Lett.*, vol. 23, no. 16, pp. 1136–1138, 2011.
- [4] J.-N. Guo, J. Zhang, Y.-Y. Zhang, G. Xin, and L. Li, "Constant weight space-time codes for dimmable MIMO-VLC systems," *IEEE Photon. J.*, vol. 12, no. 6, pp. 1–15, 2020.
- [5] O. P. Babalola and V. Balyan, "Constant weight polar coded orthogonal space-time block codes for dimmable indoor MIMO-VLC systems," *IEEE Commun. Lett.*, vol. 26, no. 10, pp. 2395–2399, 2022.
- [6] O. P. Babalola and V. Balyan, "Dimmable constant weight polar-coded non-orthogonal multiple access with orthogonal space-time block coding visible light communication systems," *IET Commun.*, vol. 18, no. 17, pp. 1071–1078, 2024.
- [7] I. S. C. Rodrigues, L. R. Ximenes, and R. Arthur, "Space-time-color (STC) scheme with symbol-hopping for color shift keying (CSK) modulation," *IEEE Commun. Lett.*, vol. 26, no. 2, pp. 369–373, 2022.
- [8] A. L. F. de Almeida, G. Favier, and J. C. M. Mota, "PARAFAC-based unified tensor modeling for wireless communication systems with application to blind multiuser equalization," *Signal Processing*, vol. 87, no. 2, pp. 337–351, 2007.
- [9] A. L. F. de Almeida, G. Favier, and J. C. M. Mota, "A constrained factor decomposition with application to MIMO antenna systems," *IEEE Transactions on Signal Processing*, vol. 56, no. 6, pp. 2429–2442, 2008.
- [10] G. Favier, M. N. da Costa, A. L. de Almeida, and J. M. T. Romano, "Tensor spacetime (TST) coding for MIMO wireless communication systems," *Signal Process.*, vol. 92, no. 4, pp. 1079–1092, 2012.
- [11] G. Favier and A. L. F. de Almeida, "Overview of constrained PARAFAC models," *EURASIP J. Adv. Signal Process.*, vol. 2014, no. 142, 9 2014.
- [12] L. R. Ximenes, B. A. Laredo, and R. Arthur, "Integrated data detection and video restoration for optical camera communications," *Digit. Signal Process.*, vol. 141, p. 104192, 2023.
- [13] L. R. Ximenes and M. F. Alves, "Tensor-based screen-to-camera communications," *IEEE Commun. Lett.*, pp. 1–1, 2023.
- [14] L. R. Ximenes, P. Gonçalves, M. F. Alves, and R. Arthur, "Achieving super-resolution reconstruction in optical camera communications," in *19th Int. Symp. Wireless Commun. Syst. (ISWCS)*, 2024, pp. 1–6.
- [15] L. R. Ximenes, G. Favier, and A. L. F. de Almeida, "Semi-blind receivers for non-regenerative cooperative MIMO communications based on nested parafac modeling," *IEEE Transactions on Signal Processing*, vol. 63, no. 18, pp. 4985–4998, 2015.
- [16] G. T. de Araújo and A. L. F. de Almeida, "PARAFAC-based channel estimation for intelligent reflective surface assisted MIMO system," in *Proc. Sensor Array and Multich. Signal Process. Workshop (SAM)*, 2020.
- [17] G. T. de Araújo, A. L. F. de Almeida, and R. Boyer, "Channel estimation for intelligent reflecting surface assisted MIMO systems: A tensor modeling approach," *IEEE J. Sel. Topics Signal Process.*, vol. 15, no. 3, pp. 789–802, 2021.
- [18] K. Ardah, S. Gharekhloo, A. L. F. de Almeida, and M. Haardt, "TRICE: A channel estimation framework for RIS-aided millimeter-wave MIMO systems," *IEEE Signal Process. Lett.*, vol. 28, pp. 513–517, 2021.
- [19] R. Singh, T. O'Farrell, and J. P. R. David, "An enhanced color shift keying modulation scheme for high-speed wireless visible light communications," *J. Lightw. Technol.*, vol. 32, no. 14, pp. 2582–2592, 2014.
- [20] R. A. Harshman and M. E. Lundy, "PARAFAC: Parallel factor analysis," *Comput. Statist. & Data Anal.*, vol. 18, no. 1, pp. 39–72, 1994.
- [21] J. B. Kruskal, "Three-way arrays: Rank and uniqueness of trilinear decompositions, with application to arithmetic complexity and statistics," *Linear Algebra and its Appl.*, vol. 18, no. 2, pp. 95–138, 1977.
- [22] "IEEE recommended practices for modulating current in high-brightness leds for mitigating health risks to viewers," *IEEE Std 1789-2015*, pp. 1–80, 2015.